Bridges of Periodic Solutions and Tori in Semiconductor Lasers Subject to Delay

D. Pieroux and T. Erneux
Université Libre de Bruxelles, Optique Nonlinéaire Théorique, Campus Plaine, C.P. 231, 1050 Bruxelles, Belgium

B. Haegeman, K. Engelborghs, and D. Roose
Department of Computer Science, K.U. Leuven, Celestijnenlaan 200A, 3001 Heverlee, Belgium
(Received 5 January 2001; published 22 October 2001)

For semiconductor lasers subject to a delayed optical feedback, branches of steady states sequentially appear as the feedback rate is increased. But branches of time-periodic solutions are connecting pairs of steady states and provide bridges between stable and unstable modes. All bridges experience a change of stability through a torus bifurcation point. Close to the bifurcation point, the torus remains localized near a specific fixed point in phase space. As the feedback rate increases, the torus envelope suddenly unfolds and its trajectory visits two or more unstable fixed points, anticipating the rich dynamics observed at larger feedback rates.

DOI: 10.1103/PhysRevLett.87.193901 PACS numbers: 42.60.Mi, 42.55.Px

Nonlinear problems with a delayed feedback appear in many areas of science and engineering. They are modeling problems in chemistry (diffusion through a membrane, illuminated thermochemical reaction [1]), in biology (blood cell production [2,3], neural control [4], respiratory physiology [5]), in the medical sciences (drug delivery [6]), in mechanics (ship rolling [7]), as well as many other physical problems [8]. In nonlinear optics, a delayed feedback often plays an active role in the device. It may be used to stabilize a laser [9] or to deliberately produce a chaotic output [10]. It may also considerably diminish the performances of semiconductor lasers. These lasers appear in many applications (laser printer, CD player, code bar reading at the supermarket) and are highly sensible to delayed optical feedback. A weak optical feedback from external reflectors such as the front facet of an optical fiber, a mirror, or an optical disk is enough to destabilize the normal output of the laser.

For lasers controlled by feedback or subject to an unwanted feedback as well as other physical or biological systems modeled by delay-differential equations, the delay may have a stabilizing or a destabilizing effect. In many cases, however, we observe cascading instabilities which lead to complex dynamical regimes. Combined analytical and numerical studies of delay-differential equations (DDE) remain rare and it is not surprising that a lot of the current efforts on DDE concentrate on specific problems in nonlinear optics. In particular, a semiconductor laser subject to a delayed optical feedback is a key problem for all semiconductor laser devices. Most of our understanding of its behavior comes from numerical studies [11] . One interesting dynamical regime, called low frequency fluctuation or LFF, has attracted a lot of attention. If a semiconductor laser operates close to its threshold, the laser power exhibits irregular oscillations with short and long time scales. The long time scale is about 100 ns and is characterized by sudden intensity dropouts. The short time scale is of the order of 100 ps and is much harder to identify [12]. Recent experimental investigations have considerably contributed to our understanding of LFF: a stable steady state mode of operation called the maximum gain mode always exists as an alternate to LFF [13] and LFF appears gradually as the number of modes increases [14]. Theoretically, new ideas have also appeared. We may benefit from the fact that LFF appears with a low number of modes and investigate the bifurcation diagram analytically [15]. We may simulate the laser equations for a large range of values of the physical parameters and find conditions for which LFF is almost time periodic (locked states [16]). Last, we may look for simplified forms of the laser equations which produce outputs close to LFF [17,18].

As the feedback rate is progressively increased from zero, branches of steady-state intensities appear and are called external cavity modes. Each branch exhibits one of more Hopf bifurcations points which are followed by more complex bifurcations. Direct time integration of the laser equations is limited to the stable solutions. Well-known software packages for bifurcation analysis such as AUTO [19] are capable of following stable and unstable time-periodic solutions but are not available for DDE. In this Letter, we use a software package for numerical continuation and bifurcation analysis specially developed for DDE [20] and we find a simple bifurcation scenario as the feedback rate increases. Specifically, we find closed branches of periodic solutions connecting pairs of isolated steady states and torus bifurcation points which mark the beginning of richer time-dependent regimes.

A single mode semiconductor laser subject to weak optical feedback is modeled by the Lang and Kobayashi equations [21]. In dimensionless form, they are given by

$$\frac{dY}{dt} = (1 + i\alpha)YZ + \kappa \exp(-i\omega_0\tau)Y(t - \tau), \quad (1)$$

$$T\frac{dZ}{dt} = P - Z - (1 + 2Z)|Y|^2, \quad (2)$$

where Y and Z are the complex electrical field and the excess carrier number, respectively [17]. Time t is measured in units of the photon lifetime τ_p ($t \equiv t'/\tau_p$). The external round-trip time is normalized as $\tau \equiv 2L/c\tau_p$, where L is the distance laser mirror and c is the speed of light. $\omega_0 \equiv \omega\tau_p$ is the dimensionless angular frequency of the solitary laser ω, and $\kappa \equiv \gamma\tau_p$ is the normalized feedback rate. α is the linewidth enhancement factor, and $T \equiv \tau_n/\tau_p$ is the ratio of the carrier τ_n to photon lifetime τ_p. P denotes the pumping rate above threshold. For all our numerical simulations, we consider κ as the bifurcation parameter and the values of the fixed parameters are the same as in [14], i.e., $T = \tau = 10^3$, $P = 10^{-3}$, $\alpha = 4$, and $\omega_0\tau = -1$. We may simplify these equations by introducing the new variables s, E, and N defined by $s \equiv t/\tau$, $E \equiv \tau^{1/2}Y$, and $N \equiv \tau Z$. Equations (1) and (2) then become

$$\frac{dE}{ds} = (1 + i\alpha)NE + \eta \exp(-i\omega_0\tau)E(s - 1), \quad (3)$$

$$q\frac{dN}{ds} = p - N - (1 + 2\tau^{-1}N)|E|^2, \quad (4)$$

where $\eta \equiv \tau\kappa$, $p \equiv \tau P$, and $q \equiv T\tau^{-1}$. The values of the fixed parameters now are $q = 1$, $p = 1$, $\tau^{-1} = 10^{-3}$, $\alpha = 4$, $\omega_0\tau = -1$, and η is the bifurcation parameter. Equations (3) and (4) are simpler to integrate numerically because there is no more a large parameter multiplying dN/ds. We may also neglect the τ^{-1} small term and reduce the number of parameters from five to four.

A basic solution of Eqs. (3) and (4), called an external cavity mode or ECM solution, corresponds to a single frequency solution of the form

$$E = A \exp[i(\Delta - \omega_0\tau)s] \quad (5)$$

and $N = B$ where A, Δ, and B are constants. The intensity $|E|^2$ of any ECM mode solution is thus constant and equals $|A|^2$. Substituting (5) into Eqs. (3) and (4) leads to conditions for A, B, and Δ which can be analyzed. Specifically, the ECM frequency Δ satisfies the transcendental equation

$$\Delta - \omega_0\tau = -\eta[\alpha\cos(\Delta) + \sin(\Delta)] \quad (6)$$

and A, B are simply related to Δ [15,22]. By analyzing Eq. (6) in the implicit form $\eta = \eta(\Delta)$, we note that the number of ECM solutions increases with η. Except for the first ECM solution which appears at $\eta = 0$ or ECM solutions that bifurcate from $A = 0$, all ECM solutions appear by pair and emerge from limit points. One branch of solutions is always unstable (called antimode) and the other branch of solutions is stable (called mode) but may experience a change of stability through a Hopf bifurcation. Hopf bifurcation points appear on all (stable or unstable) branches but cannot be determined analytically [22].

In general, bifurcation diagrams are obtained by numerical integration of the laser equations changing gradually the feedback rate [14]. The simulations are limited to the stable regimes and require several runs with different initial conditions in order to detect isolated and/or coexisting solutions. Computations can be costly and have motivated alternative techniques such as the development of numerical continuation methods appropriate for delay-differential equations [20]. A continuation method detects Hopf bifurcation points in parameter space, follows stable or unstable branches of time-periodic solutions, and determines their stability changes. Figure 1 shows the bifurcation diagram of the steady and time-periodic solutions. Branches of periodic solutions are connecting pairs of mode-antimode solutions. These bridges start and terminate at distinct Hopf bifurcation points (shown by circles in Fig. 1). They also overlap points where a mode and an antimode admit the same intensity. In the limit of large values of q, Eqs. (3) and (4) admit mixed ECM solutions of the form

$$E \simeq A_1 \exp[i(\Delta_1 - \omega_0\tau)s] + A_2 \exp[i(\Delta_2 - \omega_0\tau)s] \quad (7)$$

in the vicinity of these points [15]. Δ_1 and Δ_2 are two single ECM frequencies satisfying Eq. (6) evaluated at the equal intensity point. Because $q = 1$, the approximation (7) is only indicative. Note from (7) that $|E|^2$ is oscillating in time with a frequency equal to $|\Delta_1 - \Delta_2|$. In Fig. 2, we consider the first bridge of periodic solutions and compare the extrema of $|E|$ using (7) with the numerically computed solution. The qualitative agreement between these solutions suggests that bridges can be understood physically as combinations of two ECMs such as (7). We also

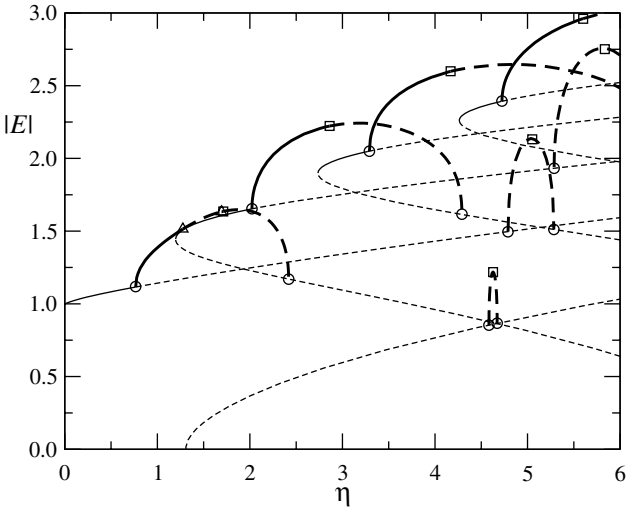

FIG. 1. Bifurcation diagram of the steady and time-periodic solutions. Full and dashed lines correspond to stable and unstable solutions, respectively. Circles, triangles, and squares denote Hopf, period doubling, and torus bifurcation points, respectively. Closed branches of periodic solutions are connecting a mode and an antimode. The first branch of periodic solutions admits a closed branch of period two solutions (not shown). A torus bifurcation point immediately follows the second period doubling bifurcation point ($T = \tau = 10^3$, $P = 10^{-3}$, $\alpha = 4$, and $\omega_0\tau = -1$).

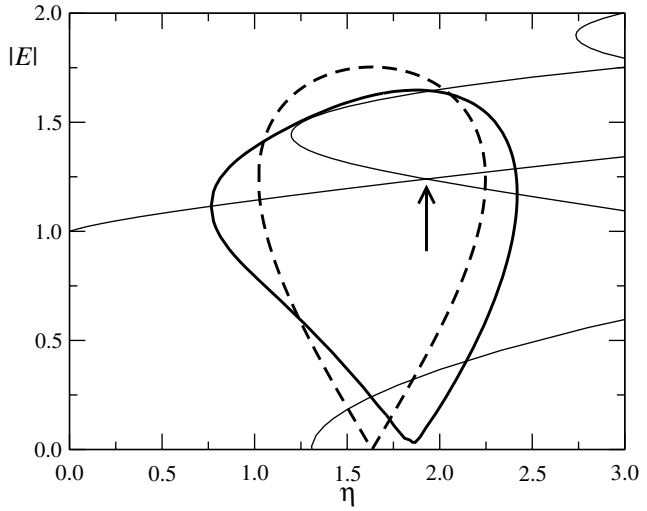

FIG. 2. First branch of periodic solutions. Both the maxima and the minima of the oscillations are shown. The numerical branch (full line) is compared to the approximation in [15] (dashed line). It is given by (7) where Δ_1 and Δ_2 are the single mode ECM frequencies evaluated at the equal intensity point (shown in the figure by an arrow). Values of the parameters are the same as in Fig. 1.

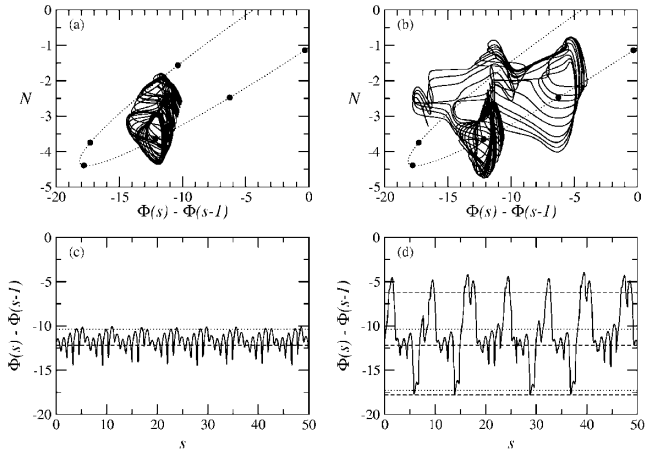

FIG. 3. Tori. At a critical feedback rate, a torus oscillating near an unstable periodic orbit suddenly unfolds into a more complex regime. This new regime dominates at higher values of η but coexists with the previous torus for a very small domain of η. The solutions are represented in the phase plane N vs $\Phi(s-1) - \Phi(s)$. We also show $\Phi(s-1) - \Phi(s)$ as a function of time s. Here $\Phi \equiv \phi + \omega_0 \tau s$, where ϕ is defined as the phase of the complex electrical field E. All the ECM solutions (Δ, B) are fixed points in the phase plane and are located on an ellipse given by $\Delta = \omega_0\tau + \alpha N \pm \sqrt{\eta^2 - N^2}$. Moreover, the broken lines in the $\Phi(s-1) - \Phi(s)$ vs s diagram correspond to specific ECM frequencies Δ. Values of the parameters are the same as in Fig. 1 and $\eta = 4.4$. In (a), the torus has been obtained by progressively increasing η from a lower value. In (b), the torus has been obtained by progressively decreasing η from a larger value.

note from Fig. 1 the existence of secondary torus bifurcation points (squares in Fig. 1). These bifurcations are important for the high intensity branches because they mark their change of stability and their transition to more complex regimes.

It is worthwhile to investigate the behavior of the tori as they emerge from their bifurcation points. To this end, we use a standard integration technique and solve numerically Eqs. (3) and (4). We concentrate on the high intensity branches. As the feedback rate surpasses the torus bifurcation point, the oscillations are quasiperiodic and the envelope of the tori remains localized in the vicinity of the original ECM point (see Fig. 3a). The oscillations are typically quasiperiodic, i.e., a low frequency modulation of rapid oscillations (see Fig. 3c). The period of the rapid oscillations is $\mathrm{Pe} \simeq 1.16$ which is close to the analytical estimate $\mathrm{Pe} = 2\pi/|\Delta_2 - \Delta_1| \simeq 1.14$ (here, $\Delta_1 \simeq -17.5$ and $\Delta_2 \simeq -12$ are the frequencies of the two interacting ECMs). Our bifurcation scenario substantiates earlier investigations on high frequency regimes possibly linked to a mode-antimode interaction [23]. The period of the slow envelope is about $\mathrm{Pe} \simeq 6.25$ and manifests the effect of the laser relaxation oscillations corrected by the feedback [22]. Above a critical feedback rate, we note a sudden jump to a quite different regime. Specifically, the torus envelope unfolds into a trajectory that is now orbiting near two or more ECM points (see Fig. 3b). The time evolution shown in Fig. 3d indicates that several unstable single mode or unstable periodic orbits are visited. The common feature between these modes and orbits is that they admit a similar value of N (see Fig. 3b). A detailed numerical analysis of the solutions near the transition point between bounded and unbounded tori indicates a slight domain of hysteresis.

The multifrequency regime appearing as the bounded torus unfolds in the phase plane anticipates the rich dynamics of LFF observed at larger feedback rates. The bifurcation scenario (periodic isola, torus bifurcation, and torus unfolding) repeats itself for each high intensity branch of periodic solutions introducing more periodic orbits and allowing the progressive development of a mature LFF observed at larger values of the feedback rate.

Because bridges of pulsating intensity solutions become unstable as the feedback parameter increases, high frequencies resulting from the beating of two ECMs are difficult to observe experimentally under normal LFF conditions (i.e., low pump, low feedback, and large external cavity conditions). They are more likely to be observed for short cavity experiments [23], and recent work suggests that regular periodic regimes are possible [24]. From a theoretical point of view, a laser subject to two optical feedbacks [25] or exhibiting two polarizations [26] are interesting problems because they admit a larger number of ECMs meaning better chances to observe stable bridges.

This research was supported by the European Office of Aerospace Research Laboratory, Air Force Office of Scientific Research, Air Force Research Laboratory, under Contract No. F61775-00-WE021, the National Science

Foundation Grant No. DMS-9973203, the Research Council K. U. Leuven (Project No. OT/98/16), the FNRS and FWO (Belgium), and the programme on Interuniversity Poles of Attractions for Science, Technology and Culture (IUAP P4/02 and IUAP P4/07).

[1] I. R. Epstein and J. A. Pojman, *An Introduction to Nonlinear Chemical Dynamics* (Oxford University Press, New York, 1998).

[2] M. C. Mackey and L. Glass, Science **197**, 287 (1977); L. Glass and M. C. Mackey, Ann. N.Y. Acad. Sci. **316**, 214 (1979).

[3] J. D. Murray, *Mathematical Biology,* Biomathematics Texts Vol. 19 (Springer-Verlag, Berlin, 1980).

[4] A. Longtin and J. G. Milton, Math. Biosci. **90**, 183 (1988); Bull. Math. Biol. **51**, 605 (1989); A. Longtin, J. G. Milton, and M. C. Mackey, Phys. Rev. A **41**, 6992 (1990).

[5] A. C. Fowler, *Mathematical Models in the Applied Sciences,* Cambridge Texts in Applied Mathematics (Cambridge University Press, Cambridge, 1997).

[6] J. G. Milton, S. A. Campbell, and J. Bélair, J. Biol. Syst. **3**, 711 (1995).

[7] N. Minorsky, *Nonlinear Oscillations* (D. Van Nostrand Co., Inc., Princeton, 1962).

[8] R. D. Driver, *Ordinary and Delay Differential Equations,* Applied Mathematical Sciences Vol. 20 (Springer-Verlag, Berlin, 1977).

[9] D. J. Gauthier, D. W. Sukow, H. M. Concannon, and J. E. S. Socolar, Phys. Rev. E **50**, 2343 (1994); J. E. S. Socolar, D. W. Sukow, and D. J. Gauthier, Phys. Rev. E **50**, 3245 (1994); S. Bielawski, D. Derozier, and P. Glorieux, Phys. Rev. E **49**, R971 (1994).

[10] J.-P. Goedgebuer, L. Larger, and H. Porte, Phys. Rev. E **57**, 2795 (1998); L. Larger, J.-P. Goedgebuer, and J.-M. Merolla, IEEE J. Quantum Electron. **34**, 594 (1998).

[11] G. H. M. van Tartwijk, A. M. Levine, and D. Lenstra, IEEE J. Sel. Top. Quantum Electron. **1**, 466 (1995); J. Mork, B. Tromborg, and J. Mark, IEEE J. Quantum Electron. **28**, 93 (1992); T. Sano, Phys. Rev. A **50**, 2719 (1994); C. Masoller and N. B. Abraham, Phys. Rev. A **57**, 1313 (1998); R. L. Davidchack, Y.-C. Lai, A. Gavrielides, and V. Kovanis, Physica (Amsterdam) **145D**, 130 (2000).

[12] I. Fischer and G. H. M. van Tartwijk, A. M. Levine, and W. Elsässer, E. Göbel, and D. Lenstra, Phys. Rev. Lett. **76**, 220 (1996).

[13] T. Heil, I. Fischer, and W. Elsässer, Phys. Rev. A **58**, R2672 (1998).

[14] A. Hohl and A. Gavrielides, Phys. Rev. Lett. **82**, 1148 (1999).

[15] T. Erneux, F. Rogister, A. Gavrielides, and V. Kovanis, Opt. Commun. **183**, 467 (2000).

[16] A. Gavrielides, T. C. Newell, V. Kovanis, R. G. Harrison, N. Swanston, D. Yu, and W. Lu, Phys. Rev. A **60**, 1577 (1999).

[17] P. M. Alsing, V. Kovanis, A. Gavrielides, and T. Erneux, Phys. Rev. A **53**, 4429 (1996).

[18] G. Huet, P. A. Porta, S. P. Hegarty, J. G. McInerney, and F. Holland, Opt. Commun. **180**, 339 (2000).

[19] E. Doedel, T. Fairgrieve, B. Sandstede, A. Champneys, Yu. Kuznetsov, and X. Wang, "AUTO 97: Continuation and bifurcation software for ordinary differential equations" (http://indy.cs.concordia.ca/auto/main.html).

[20] K. Engelborghs, T. Luzyanina, K. in't Hout, and D. Roose, SIAM J. Sci. Comp. **22**, 1593 (2000); K. Engelborghs, T. Luzyanina, and D. Roose, J. Comp. Appl. Math. (to be published); K. Engelborghs, "DDE-BIFTOOL: a Matlab package for bifurcation analysis of delay differential equations" (http://www.cs.kuleuven.ac.be/~koen/delay/ddebiftool.shtml).

[21] R. Lang and K. Kobayashi, IEEE J. Quantum Electron. **16**, 347 (1980).

[22] G. Lythe, T. Erneux, A. Gavrielides, and V. Kovanis, Phys. Rev. A **55**, 4443 (1997).

[23] A. A. Tager and B. B. Elenkrig, IEEE J. Quantum Electron. **29**, 2886 (1993); A. A. Tager and K. Petermann, IEEE J. Quantum Electron. **30**, 1553 (1994).

[24] T. Heil, I. Fischer, and W. Elsäßer, and A. Gavrielides (to be published).

[25] F. Rogister and P. Mégret, O. Deparis, M. Bondel, and T. Erneux, Opt. Lett. **24**, 1218 (1999).

[26] H. Li, A. Hohl, A. Gavrielides, H. Huo, and K. D. Choquette, Appl. Phys. Lett. **72**, 2355 (1998).